



Anal. Bioanal. Chem. Res., Vol. 6, No. 1, 125-136, June 2019.

Facile Hydrothermal Synthesis of Magnetic Sepiolite Clay for Removal of Pb(II) from Aqueous Solutions

Maryam Fayazi

Department of Environment, Institute of Science and High Technology and Environmental Sciences, Graduate University of Advanced Technology, Kerman, Iran

(Received 20 July 2018, Accepted 4 October 2018)

The sepiolite-iron oxide nanocomposite (Sepiolite-Fe₃O₄) was synthesized *via* facile hydrothermal method and used as an efficient magnetic adsorbent for removal of Pb(II) ions from water samples. The Sepiolite-Fe₃O₄ nanocomposite was characterized by X-ray diffraction (XRD), Fourier transform infrared spectroscopy (FTIR), transmission electron microscopy (TEM), vibration sample magnetometer (VSM) and scanning electron microscopy (SEM) techniques. The equilibrium data were tested using different isotherm models including Langmuir, Freundlich and Temkin. The adsorption isotherm fits well with the Langmuir model and the maximum Pb(II)-sorption capacity of 96.15 mg g⁻¹ was calculated at room temperature. Kinetic data were well interpreted with the pseudo-second-order model ($R^2 > 0.9998$), suggesting that the adsorption process was controlled by chemical reactions. The as-prepared magnetic adsorbent was easily reused through sequential adsorption-desorption cycles, indicating that the Sepiolite-Fe₃O₄ nanocomposite has an acceptable stability and reusability. As a result, this study indicates that the novel adsorbent nanocomposite may be an ideal adsorbent for heavy metal-contaminated water treatment.

Keywords: Lead removal, Sepiolite, Magnetic nanocomposite, Adsorption, Heavy metals

INTRODUCTION

In recent years, water pollution by heavy metal ions has been a widespread environmental problem because of non-biodegradability, accumulation in environment and living body, discharge and harmful effects of these heavy metals [1]. Heavy metals are mostly originated from industrial activities resulting in the release of toxic metals into the environment directly or indirectly, reaching the air, soil and water sources [2-5]. Lead (Pb) and its compounds can result in damage of living organisms, depending on the level and duration of exposure [6,7]. Therefore, removal of toxic lead ions prior to disposal is very important task. Various conventional methods have been proposed for the lead treatment such as chemical precipitation [8], electrochemical

method [9], biological method [10], ion-exchange [11], membrane filtration [12] and adsorption [13]. Among these techniques, adsorption process has been frequently applied for heavy metal ions removal from water samples due to the convenience in design, application, and reuse of sorbent materials [14].

During the past few years, the naturally clay minerals such as bentonite, montmorillonite, palygorskite, kaolinite and sepiolite have been used for the adsorption of organic dyes and metals from aqueous solutions [15-22]. Sepiolite is a 2:1 type of layered and fibrous mineral with molecular size channels [23]. It is a non-swelling, lightweight, porous clay mineral with a unit cell formula of Si₁₂Mg₈O₃₀(OH)₄(OH₂)₄·8H₂O. Special properties of sepiolite such as large specific surface area, numerous abundance, low cost, chemical and mechanical constancy, and well adsorption ability have made it an appropriate

*Corresponding author. E-mail: m.fayazi@kgut.ac.ir

mineral for removing heavy metals [24]. However, the difficulty of separating sepiolite from water limits its practical application.

Magnetic nanoparticles (MNPs) as effective sorbents with large surface area and high magnetic susceptibility have been identified [25]. Therefore, we expect that the combination of sepiolite and Fe₃O₄ can provide a magnetic hybrid with great uptake capacity that can overcome some disadvantages of Fe₃O₄ such as agglomeration and chemical instability in acidic media.

The present study is aimed at the preparation of the sepiolite-iron oxide nanocomposite (Sepiolite-Fe₃O₄) *via* hydrothermal method. The prepared nanocomposite is characterized by variety of methods. The adsorption kinetics and isotherms are derived. Desorption and recyclability of the nanocomposite adsorbent are also investigated.

EXPERIMENT

Reagents

The natural sepiolite used for this study came from Fariman (Iran). Other chemical reagents including FeCl₂·4H₂O, Pb(NO₃)₂ and NH₄OH (25%, w/w) were of analytical grade from Merck (Darmstadt, Germany). The standard solution of Pb(II) ions (1000 mg l⁻¹) was prepared by dissolving an appropriate amount of lead nitrate in Milli-Q water.

Apparatus

A Varian Spectra AA 220 (Varian, Melbourne, Australia) flame atomic absorption spectrometer (FAAS) was used for determination of lead content. Magnetic measurements were carried out using a vibrating sample magnetometer (VSM) (Model VSM-P7, Toei Industrial, Tokyo, Japan). The morphology of the Sepiolite-Fe₃O₄ nanocomposite was evaluated by scanning electron microscope (SEM, KYKY-EM 3200, Zhongguancun Beijing, China). Fourier transform infrared (FTIR) spectra were recorded on a Bruker tensor 27 spectrometer (Madison, WI, USA). Transmission electron microscopic (TEM) images were carried out by a LEO 912AB TEM (Carl Zeiss Inc., Jena, Germany). X-ray diffraction (XRD) patterns of the samples were recorded by PANalytical X-

ray diffractometer (model X'Pert PRO, Almelo, Netherlands) using monochromatic Cu K α radiation (wavelength $\lambda = 0.154$ nm).

Preparation of Sepiolite-Fe₃O₄ Nanocomposite

Before modification, the natural sepiolite was treated with Milli-Q water to eliminate the soluble impurities. The resulting supernatant was filtered and then dried at 105 °C for 24 h. The Sepiolite-Fe₃O₄ was prepared *via* simple hydrothermal method. In a typical synthesis, 2.5 g of the purified sepiolite sample was added into a 40 ml solution of 6.5 g FeCl₂·4H₂O and sonicated for 10 min. After that, 31 ml of NH₄OH solution was added to above suspension with vigorous stirring. Afterwards, the mixed suspension was transferred into a Teflon lined hydrothermal autoclave (200 ml capacity) and then heated at 140 °C for 4 h. In final step, the product (Sepiolite-Fe₃O₄) was separated by a magnet, washed repeatedly with deionized water and then dried at 60 °C for 24 h.

Batch Adsorption Studies

Adsorption tests were performed in Erlenmeyer flasks (50 ml) where 20 ml of Pb(II) solutions at desired concentration and pH were placed in these flasks. A certain amount of the prepared magnetic clay nanocomposite was added to each flask and set in an incubator shaker of 200 rpm at 24 ± 1 °C for a desired contact time. Finally, the magnetic adsorbent was separated by a magnet, and the concentration of residual Pb(II) in the solutions was measured by FAAS. Each experiment was duplicated under identical conditions. The affinity of the Sepiolite-Fe₃O₄ toward Pb(II) ions can be expressed in terms of the distribution coefficient. The specific amount of adsorbed Pb(II) per unit mass of the adsorbent, the removal efficiency and distribution coefficient were calculated from the following relationships [26]:

$$q_e = \frac{(C_i - C_e)V}{m} \quad (1)$$

$$K_d = \frac{C_i - C_e}{C_e} \times \frac{V}{m} \quad (2)$$

$$\% \text{ Removal} = \frac{C_i - C_e}{C_i} \times 100 \quad (3)$$

where q_e (mg g^{-1}) is the equilibrium adsorption capacity, K_d (l g^{-1}) is distribution coefficient, C_i and C_e (mg l^{-1}) are the initial and equilibrium concentrations of Pb(II) in aqueous solution, respectively, V (l) is the volume of Pb(II) solution and m (mg) is the amount of sorbent.

Kinetic experiments for Pb(II) ions at adsorption times (2-150 min) were conducted. For each experiment, 50 mg of the sorbent was weighed and added into 20 ml of Pb(II) ions solution (50 mg l^{-1}). The kinetic behavior of Pb(II) ions was studied on the basis of Lagergren's pseudo-first-order and pseudo-second-order models given by the following equations (Eq. (4) and Eq. (5)) [27,28]:

pseudo-first-order

$$\ln(q_e - q_t) = \ln q_e - k_1 t \quad (4)$$

pseudo-second-order

$$\frac{t}{q_t} = \frac{1}{k_2 q_e^2} + \frac{1}{q_e} t \quad (5)$$

where q_e and q_t (mg g^{-1}) are the adsorption capacities at equilibrium and at time t , respectively, and k_1 and k_2 are the pseudo-first-order (min^{-1}) and pseudo-second-order ($\text{g mg}^{-1} \text{min}^{-1}$) rate constants.

Adsorption isotherms were established at various initial concentrations (10-500 ppm) of Pb(II) ions. The solution was stirred for 1 h at fixed amount of sorbent (50 mg), and the final concentration for Pb(II) ions was determined by FAAS analysis. Three adsorption models (the Langmuir, Freundlich, and Temkin isotherms) were used to describe the equilibrium adsorption data. The Langmuir adsorption isotherm model is the description of monolayer adsorption on an energetically uniform surface with finite adsorption sites. The linear form of Langmuir model is given by Eq. (6) [29]:

$$\frac{C_e}{q_e} = \frac{1}{k_1 q_m} + \frac{1}{q_m} C_e \quad (6)$$

where C_e is the concentration of Pb(II) solution at equilibrium (mg l^{-1}), q_e is the amount of Pb(II) ions per mass of adsorbent at equilibrium (mg g^{-1}), k_1 is the Langmuir constant (l mg^{-1}) that represents the affinity between solute

and adsorbent, and q_m is the maximum adsorption capacity at monolayer coverage (mg g^{-1}).

The Freundlich isotherm model is an empirical equation based on the assumption of heterogeneous adsorption that is suitable to describe both monolayer and multilayer adsorption. The Freundlich isotherm is expressed in Eq. (7) [30]:

$$\ln q_e = \ln K_f + \frac{1}{n} \ln C_e \quad (7)$$

where K_f ($\text{mg g}^{-1} (\text{l mg}^{-1})^{1/n}$) and n are the Freundlich constants related to the adsorption capacity and sorption intensity of the sorbent, respectively. The Temkin isotherm was also applied to the adsorption of Pb(II) ions on Sepiolite- Fe_3O_4 . The Temkin isotherm assumes uniform distribution of heterogeneous binding sites and an adsorption enthalpy that varies due to the heterogeneity of sites. This model is presented as [31]:

$$q_e = B_t \ln K_t + B_t \ln C_e \quad (8)$$

where K_t and B_t are the Temkin constants related to the initial adsorption heat and the surface heterogeneity of the adsorbent, respectively. One of the important features of Langmuir isotherm can be mentioned using the dimensionless separation factor (R_L), which is given by [32]:

$$R_L = \frac{1}{1 + K_1 C_i} \quad (9)$$

where k_1 (l mg^{-1}) is the Langmuir constant and C_i (mg l^{-1}) is the initial Pb(II) concentration. The R_L values in the range of 0-1 demonstrate favorable adsorption [33].

RESULTS AND DISCUSSION

Characterization

FTIR spectra of the purified sepiolite and Sepiolite- Fe_3O_4 nanocomposite are recorded in Fig. 1. The bands at 3437 and 1662 cm^{-1} are respectively assigned to the OH stretching, representing the zeolitic water in the channels and bound water coordinated to magnesium in the octahedral sheet. The absorption peaks at 1211 and

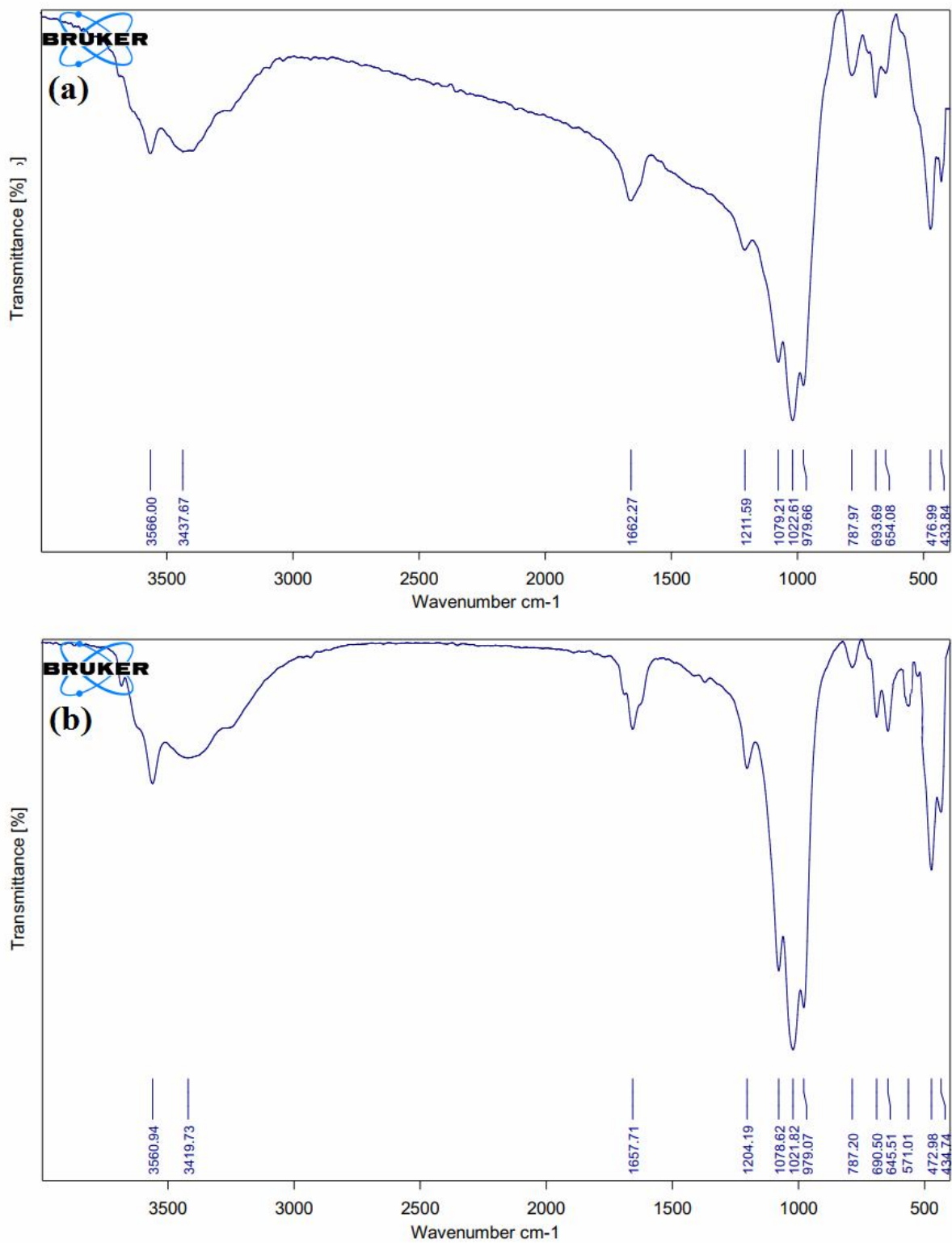


Fig. 1. FTIR spectra of (a) sepiolite, and (b) the Sepiolite-Fe₃O₄ nanocomposite.

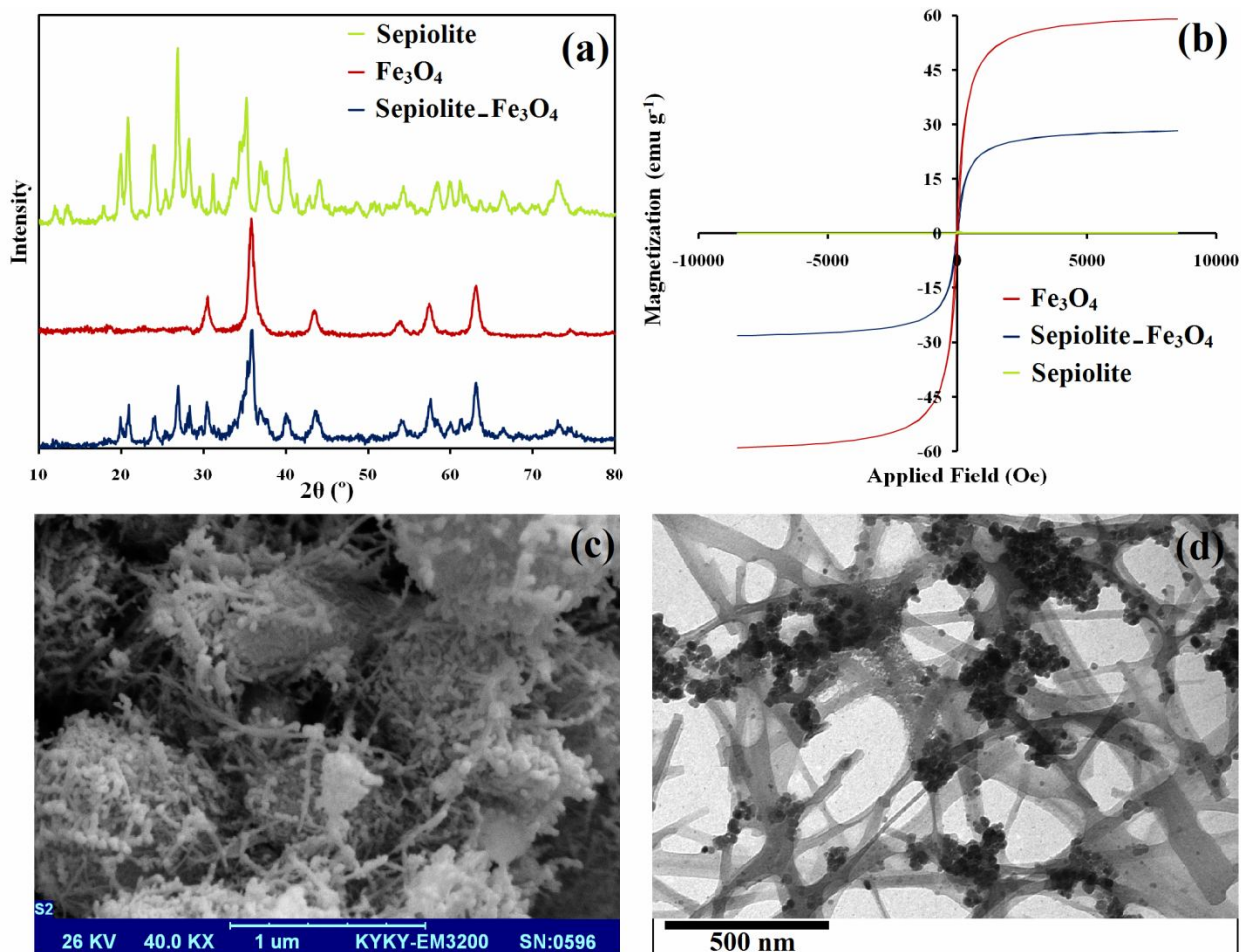


Fig. 2. (a) XRD patterns of sepiolite, Fe₃O₄, and Sepiolite-Fe₃O₄. (b) VSM magnetization curves of sepiolite, Fe₃O₄, and Sepiolite-Fe₃O₄. (c) SEM and (d) TEM images of the prepared Sepiolite-Fe₃O₄ nanocomposite.

1022 cm⁻¹ represent the stretching of Si-O in the Si-O-Si groups of the tetrahedral sheet [34]. A band at 433 cm⁻¹, originated from Si-O-Mg groups, and bands at 693 and 654 cm⁻¹ can be also assigned to vibrations of the Mg-OH bond [35]. In Sepiolite-Fe₃O₄ sample, the absorption band at 571 cm⁻¹ indicates the Fe-O vibrations of Fe₃O₄ nanoparticles [36].

Figure 2a represents XRD patterns of sepiolite, Fe₃O₄ and Sepiolite-Fe₃O₄ nanocomposite. In sepiolite sample, the peaks can be indexed to 19.92 (060), 20.77 (131), 23.95 (260), 26.77 (080), 35.20 (371), 36.91 (202), 40.12 (541) and 60.21° (791) as planes of a cubic unit cell of sepiolite based on comparison with the standard pattern of

sepiolite (JCPDS card No. 13-0595). [37]. In Fe₃O₄ sample, six well-resolved diffraction peaks located at 30.45°, 35.81°, 43.31°, 53.69°, 57.44° and 62.95° can be respectively indexed to the (220), (311), (400), (422), (511) and (440) planes of Fe₃O₄ (JCPDS 75-0449) [36]. All diffraction peaks of Fe₃O₄ matched well with the Sepiolite-Fe₃O₄ pattern, indicating that Fe₃O₄ particles have been loaded on the surface of sepiolite fibers. Furthermore, the relative intensity of the Sepiolite-Fe₃O₄ sample was reduced. These demonstrate the successful integration of magnetite particles on the surface of sepiolite fibers.

The magnetic hysteresis curve of sepiolite, Fe₃O₄ and Sepiolite-Fe₃O₄ samples, at room temperature, is exhibited

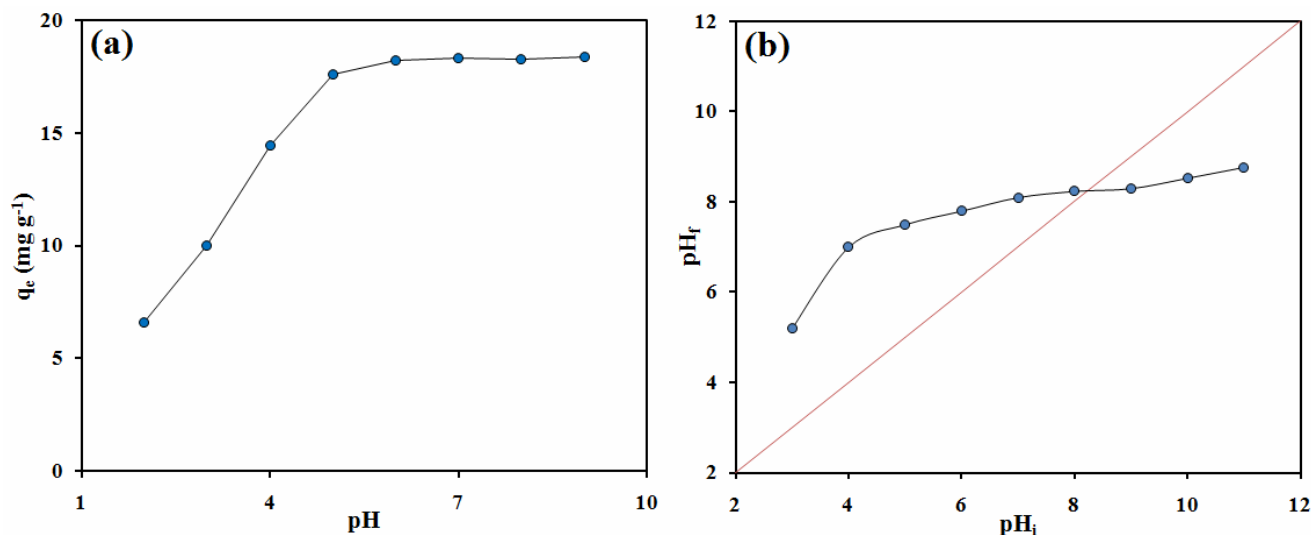


Fig. 3 (a) Effect of pH on the removal efficiency of Sepiolite-Fe₃O₄ for Pb(II) ions. Conditions: concentration of Pb(II) = 50 mg l⁻¹, sorbent dosage = 0.05 g, and time = 60 min. (b) The change in pH_{final} as a function of pH_{initial} during the equilibration of 0.05 g of Sepiolite-Fe₃O₄ with 25 ml KNO₃ (0.01 M).

in Fig. 2b. From the hysteresis loops, saturation magnetization (M_s) values for Fe₃O₄ and Sepiolite-Fe₃O₄ samples were found to be 58.9 and 28.1 emu g⁻¹, respectively. Moreover, remanent magnetization of Sepiolite-Fe₃O₄ was found to be very close to zero, indicating a nearly super-paramagnetic characteristic. Therefore, Sepiolite-Fe₃O₄ nanocomposite is a magnetic material that can be removed from solution by magnetic field.

The morphology of Sepiolite-Fe₃O₄ was characterized by SEM as indicated in Fig. 2c. As can be seen, sepiolite clay has a fibrous structure that Fe₃O₄ nanoparticles are well placed on its surface. The TEM image of the magnetic clay adsorbent is shown in Fig. 2d. It can be seen that the sepiolite presents in the form of dispersive fibers with a high length-diameter ratio, and the Fe₃O₄ nanoparticles with a diameter of 10-55 nm in spherical shape are highly covered on sepiolite nanofibers. The SEM and TEM images prove the successful preparation of Sepiolite-Fe₃O₄ nanocomposite.

Influence of pH and sorption mechanism

pH is one of the vital factors controlling the extraction and adsorption of metal ions from aqueous solutions [38].

The influence of pH was studied over the range of 2-9 and the result is depicted in Fig. 3a. As can be seen, the removal efficiency of Pb(II) ions improves with increasing the solution pH from 2 to 6, and it then remained constant in the pH range of 6-9. Pb²⁺ is predominantly present at pH ≤ 6 and the removal of Pb²⁺ is mainly accomplished by adsorption process [39]. Thus, the low Pb(II) adsorption that occurs at low pH can be due to the competition between hydrogen ion and Pb(II) ions on the active sites of sorbent. The main species at pH 7-9 are Pb(OH)⁺ and Pb(OH)₂ and thus the removal of Pb(II) is possibly accomplished by simultaneous precipitation of and sorption of Pb(OH)⁺ [40,41]. Therefore, pH 6 was selected in the following experiments.

As illustrated in Fig. 3b, the value of point of zero charge (pHPZC) was around 8.2 for Sepiolite-Fe₃O₄ nanocomposite. The pHPZC as a qualitative parameter can be applied for the sorbent surface charge balance. As the solution pH increases, in the pH range above pHPZC, the number of the anionic sepiolite active sites ($\equiv\text{S-O}^-$) increases. If the solution pH decreases below 8.2, the concentration of surface species will become different; *i.e.*, the number of $\equiv\text{S-OH}_2^+$ groups increases. As the result, Pb²⁺ ions compete with the H⁺ ions for the same active site

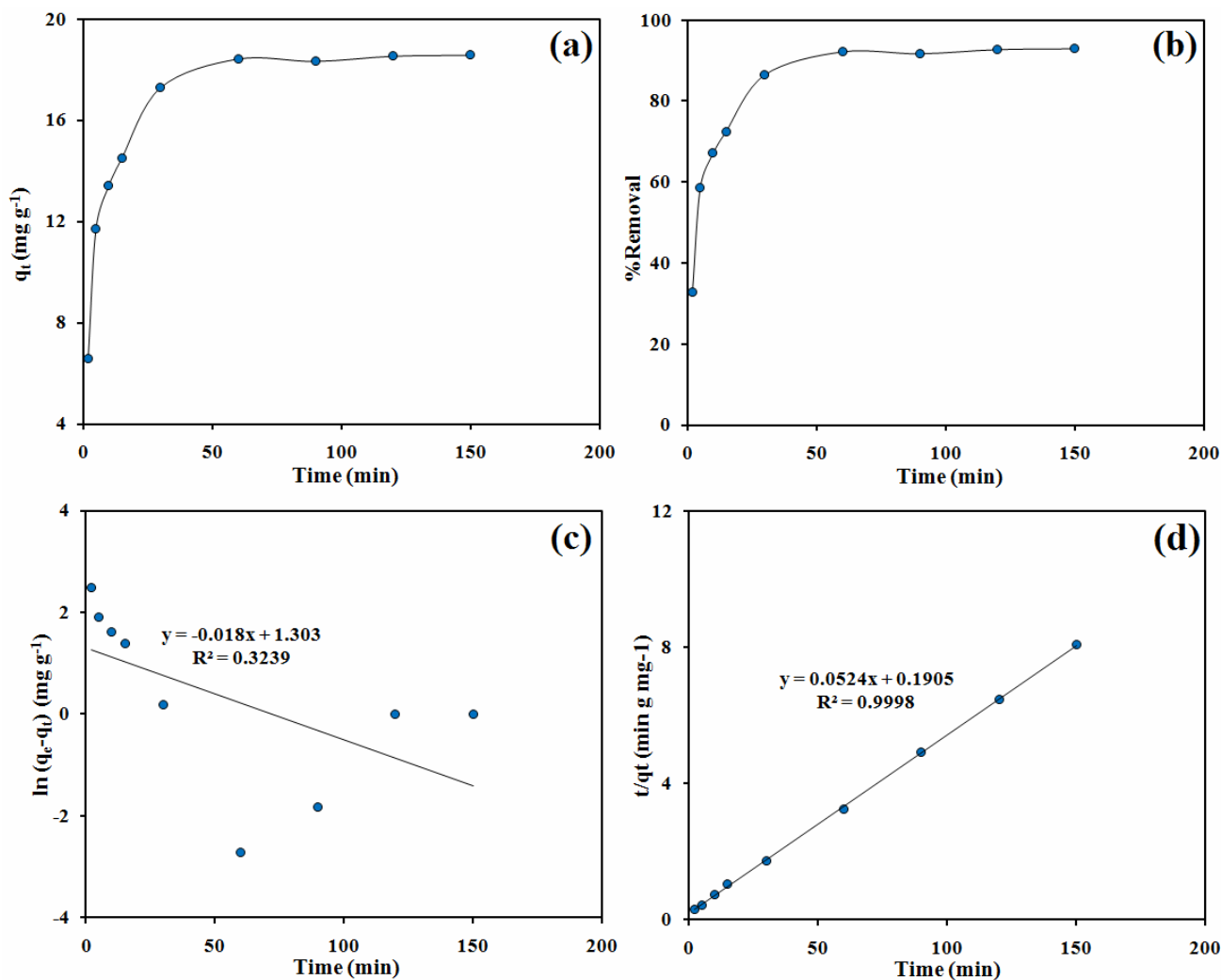


Fig. 4. (a) Effect of contact time on the removal efficiency of Sepiolite-Fe₃O₄. (b) Percentage removal as a function of time. (c) Pseudo-first order, and (d) Pseudo-second order models for adsorption of Pb(II) on the magnetic adsorbent. Conditions: concentration of Pb(II) = 50 mg l⁻¹, pH = 6.0, and sorbent dosage = 0.05 g.

(≡S-OH), resulting in surface complexation or protonation of the active surface site. Moreover, the higher affinity of the Fe₃O₄-modified sepiolite for Pb(II) sorption may be due to the presence of ≡Fe-OH groups located on the external sites of the sepiolite interacting with the Pb(II) ions.

Adsorption Kinetic

Figure 4a shows the time course of adsorption for Pb(II) ions. The adsorption capacity proceeded through a two-stage

process: initially, adsorption capacity of Pb(II) ions from solution on adsorbents was increased sharply (up 60 min) and then it became much slower and reached the plateau. The Pb(II) adsorption was also efficient (Fig. 4b) and ~92% removal with $K_d = 4.7 \times 10^3$ (ml g⁻¹) in 1 h was achieved. The experimental values were fitted to both the pseudo-first-order and pseudo-second-order kinetic models (Figs. 4c,d), and the corresponding parameters are given in Table 1. As observed, R^2 value obtained, using the pseudo-second-order kinetic model, is relatively high ($R^2 > 0.9998$), and the q_e

Table 1. Kinetic Parameters of the Pseudo-first Order and Pseudo-second Order Models for Pb(II) Sorption onto the Sepiolite-Fe₃O₄ Nanocomposite

C _i ^a	C _e ^a -1h	Removal (%)	K _d (ml g ⁻¹)	Pseudo-first-order				Pseudo-second-order		
				q _{e,exp} (mg g ⁻¹)	q _{e,cal} (mg g ⁻¹)	k ₁ (min ⁻¹)	R ²	q _{e,cal} (mg g ⁻¹)	k ₂ (g mg ⁻¹ min ⁻¹)	R ²
50	3.91	92.1	4.7 × 10 ³	18.5	3.68	0.018	0.3239	19.08	0.014	0.9998

^aAll concentrations are mg l⁻¹.

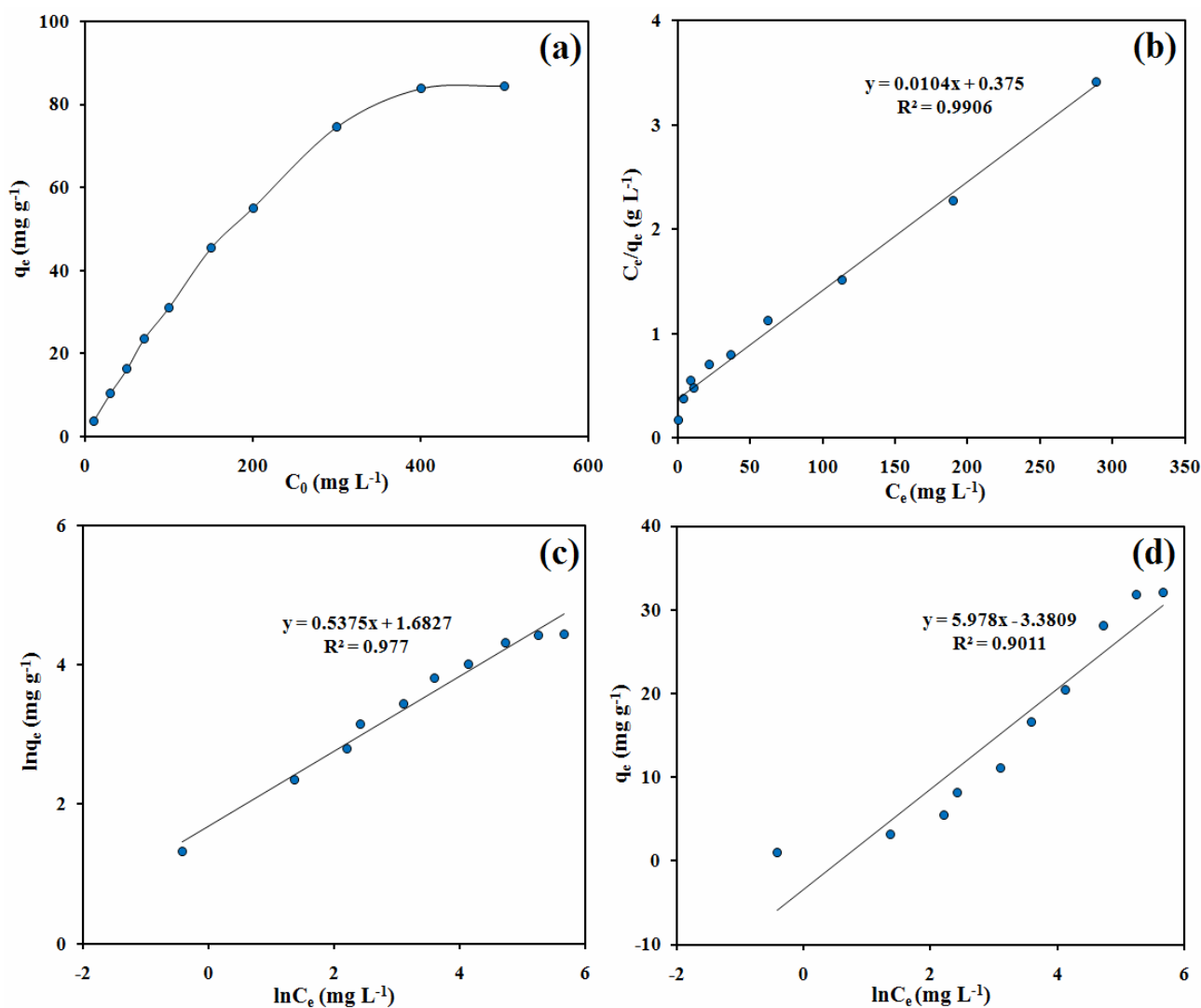


Fig. 5. (a) Adsorption isotherm of Pb(II) on the Sepiolite-Fe₃O₄. (b) Langmuir, (c) Freundlich and (d) Temkin plots for the adsorption of Pb(II) ions. Conditions: pH = 6.0, sorbent dosage = 0.05 g, and time = 60 min.

Table 2. Isotherm Parameters of Langmuir, Freundlich and Temkin Models for Pb(II) Sorption onto the Sepiolite-Fe₃O₄ Adsorbent

Langmuir isotherm				Freundlich isotherm			Temkin isotherm		
k_l (l mg ⁻¹)	q_m (mg g ⁻¹)	R^2	R_L	K_f (mg g ⁻¹ (l mg ⁻¹) ^{1/n})	n	R^2	B_t	K_t	R^2
0.028	96.15	0.9906	0.42	5.38	1.86	0.977	5.978	1.76	0.9011

Table 3. Comparative Study of Different Adsorbents for Pb(II) Adsorption

Adsorbents	Adsorption capacity (mg g ⁻¹)	Best fit isotherm	Experimental conditions	Ref.
Mangrove-alginate composite bead	10.84	Freundlich	pH = 5.0, T = 25 °C	[45]
Multi-walled carbon nanotubes/manganese oxide	19.97	-	pH = 7.0, T = 25 °C	[46]
Magnetic ion-imprinted polymer	32.58	Langmuir	pH = 6-7, T = 25 °C	[47]
Mg-Al layered double hydroxides/manganese dioxide	49.87	-	pH = 4, T = 25 °C	[48]
Aluminum oxide nanoparticles	34.10	Langmuir	pH = 5, T = 25 °C	[49]
Multi-walled carbon nanotubes/polyacrylamide	29.71	Langmuir	pH = 5.0, T = 20 °C	[50]
Diglycolamic-acid/magnetic chitosan	70.57	Langmuir	pH = 5.28	[51]
ZnO with montmorillonite	88.50	Langmuir	pH = 4.0	[52]
Gelatin-bentonite composite	47.16	Langmuir	pH = 5.34, T = 25 °C	[53]
Fly ash containing zero valent iron	78.13	-	pH = 6.0, T = 20 °C	[54]
Sepiolite-supported nanoscale zero-valent iron	44.05	Freundlich	pH = 6.0, T = 28 °C	[55]
Iron oxide coated sepiolite	75.79	Langmuir	pH = 5.5, T = 25 °C	[56]
Fe ₃ S ₄ /reduced graphene oxide composite	285.71	Langmuir	pH = 6, T = 25 °C	[57]
Porous magnesium silicate	436.68	Langmuir	pH = 5.8, T = 25 °C	[58]
NiCr layered double hydroxides (LDHs) intercalated with diphenylamine-4-sulfonate	479	Langmuir	pH = 6.0, T = 25 °C	[59]
Sepiolite-Fe ₃ O ₄	96.15	Langmuir	pH = 6.0, T = 24 °C	This work

value calculated by the same model are very close to the experimental q_e ($q_{e,exp}$) value. Therefore, the adsorption kinetic followed the pseudo-second-order adsorption kinetic model, suggesting that the adsorption of Pb(II) by Sepiolite-

Fe₃O₄ occurs through chemisorptions [42].

Adsorption Isotherm

Equilibrium isotherms are measured to determine how

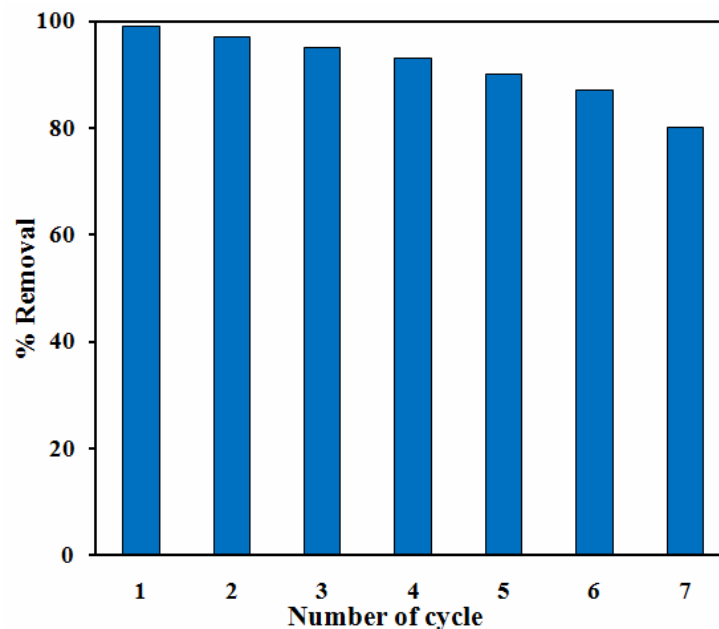


Fig. 6. Recycling of Sepiolite-Fe₃O₄ adsorbent for the removal of Pb(II) ions.

the adsorbate interacts with sorbent material [43]. The adsorption isotherm of Pb(II) ions, obtained over Sepiolite-Fe₃O₄, is shown in Fig. 5a. The Langmuir, Freundlich and Temkin isotherms for adsorption of Pb(II) ions with the Sepiolite-Fe₃O₄ nanocomposite using linear regression are displayed in Figs. 5b-d. The adsorption constants evaluated from three isotherms and their correlation coefficients are summarized in Table 2. As can be seen from Table 2, the adsorption isotherm data are well fitted the Langmuir isotherm model. Furthermore, the maximum adsorption capacity of the Sepiolite-Fe₃O₄ nanocomposite for Pb(II) based on Langmuir model (96.15 mg g⁻¹) is very close to the experimental value (84.5 mg g⁻¹). The Langmuir model presumes a monolayer of adsorbate on the outer surface of adsorbent and there is no interaction between the adsorbed molecules [44].

In this study, the calculated R_L value was found to be 0.42, suggesting that the adsorption process is favorable for Pb(II) ions by the Sepiolite-Fe₃O₄ adsorbent.

A comparison was carried out between the performance of the prepared magnetic nanocomposite with some recently reported materials [45-59] employed for Pb(II) removal in Table 3. Although the maximum adsorption capacity of some adsorbents for Pb(II) ions is higher than the Sepiolite-

Fe₃O₄ nanocomposite, some advantages of the proposed adsorbent including easy preparation, low cost and super-paramagnetic property make it a promising adsorbent for Pb(II) removal from wastewater.

Desorption and Regeneration Studies

Long term reusability of an adsorbent is another important parameter for any practical industrial application. The desorption experiments were performed after treatment of adsorbent material with 0.1 M EDTA for 1 h and the results are shown in Fig. 6. After seven repeated adsorption-desorption cycles, the removal efficiency of the Sepiolite-Fe₃O₄ nanocomposite was decreased about 20% while the adsorption properties of sorbent are still well-retained. The results demonstrated that the Sepiolite-Fe₃O₄ sorbent used in this study is an effective, economical, and stable sorbent.

CONCLUSIONS

In this study, a magnetic Sepiolite-Fe₃O₄ nanocomposite adsorbent was successfully prepared *via* one-pot hydrothermal method. The synthesized nanocomposite was then characterized by SEM, TEM, XRD, FTIR and VSM analyses. The resulting nanocomposite demonstrated

extraordinary adsorption capacity for Pb(II) ions. The adsorption data of the Sepiolite-Fe₃O₄ nanocomposite toward Pb(II) ions fit the Langmuir isotherm and follow the pseudo-second-order kinetic. The regeneration and recyclability of Sepiolite-Fe₃O₄ nanocomposite make it a greener material for heavy metal ion removal from industrial effluents. Its advantages include easy preparation, cheap and excellent adsorption properties. Also, adsorbent provides an easy separation process, because it can be isolated from the medium utilizing a magnetic field.

ACKNOWLEDGEMENTS

The author expresses their sincere gratitude to Institute of Science and High Technology and Environmental Sciences, Graduate University of Advanced Technology, Kerman, Iran for the financial support of this project (No. 3147).

REFERENCES

- [1] M.R. Moore, *Toxicol. Lett.* 148 (2004) 153.
- [2] S. Jadali, S.M. Sajjadi, H. Zavvar Mousavi, M. Rajabi, *Anal. Bioanal. Chem. Res.* 4 (2017) 171.
- [3] M. Alimohammady, M. Jahangiri, F. Kiani, H. Tahermansouri, *Res. Chem. Intermed.* 44 (2018) 69.
- [4] Z.H. Mousavi, A. HosseiniFar, V. Jahed, *J. Serb. Chem. Soc.* 77 (2012) 393.
- [5] H. Namazi, A. Heydari, A. Pourfarzolla, *Int. J. Polym. Mater. Polym. Biomater.* 63 (2014) 1.
- [6] L.H. Mason, J.P. Harp, D.Y. Han, *BioMed Res. Int.* 2014 (2014).
- [7] M. Ghanei-Motlagh, M.A. Taher, *Anal. Bioanal. Chem. Res.* 4 (2017) 295.
- [8] H. Sis, T. Uysal, *Appl. Clay Sci.* 95 (2014) 1.
- [9] A. Macías-García, M.G. Corzo, M.A. Domínguez, M.A. Franco, J.M. Naharro, *J. Hazard. Mater.* 328 (2017) 46.
- [10] R. Dobrowolski, A. Szcześ, M. Czemińska, A. Jarosz-Wikołazka, *Bioresour. Technol.* 225 (2017) 113.
- [11] X.-M. Zhang, D. Sarma, Y.-Q. Wu, L. Wang, Z.-X. Ning, F.-Q. Zhang, M.G. Kanatzidis, *J. Am. Chem. Soc.* 138 (2016) 5543.
- [12] S. Mehdipour, V. Vatanpour, H.-R. Kariminia, *Desalination* 362 (2015) 84.
- [13] H. Mousavi, A. HosseiniFar, V. Jahed, S. Dehghani, *Braz. J. Chem. Eng.* 27 (2010) 79.
- [14] F. Fu, Q. Wang, *J. Environ. Manage.* 92 (2011) 407.
- [15] W. Liu, C. Zhao, S. Wang, L. Niu, Y. Wang, S. Liang, Z. Cui, *Res. Chem. Intermed.* 44 (2018) 1441.
- [16] A. Heydari, H. Sheibani, *RSC Adv.* 5 (2015) 82438.
- [17] A. Heydari, H. Khoshnood, H. Sheibani, F. Doostan, *Polym. Adv. Technol.* 28 (2017) 524.
- [18] L. Zhu, J. Guo, P. Liu, S. Zhao, *Appl. Clay Sci.* 121 (2016) 29.
- [19] T.P.A. Shabeer, A. Saha, V.T. Gajbhiye, S. Gupta, K.M. Manjaiah, E. Varghese, *Water, Air, Soil Pollut.* 226 (2015) 41.
- [20] V. Marjanović, S. Lazarević, I. Janković-Častvan, B. Jokić, D. Janačković, R. Petrović, *Appl. Clay Sci.* 80 (2013) 202.
- [21] E. Unuabonah, K. Adebawale, B. Olu-Owolabi, *J. Hazard. Mater.* 144 (2007) 386.
- [22] Z. Hassanzadeh Siahpoosh, M. Soleimani, *Anal. Bioanal. Chem. Res.* 3 (2016) 195.
- [23] R. Donat, *J. Chem. Thermodyn.* 41 (2009) 829.
- [24] E. Ruiz-Hitzky, P. Aranda, A. Álvarez, J. Santarén, A. Esteban-Cubillo, *Advanced Materials and New Applications of Sepiolite and Palygorskite, Developments in Clay Science*, Elsevier 2011, pp. 393.
- [25] D. Afzali, M. Fayazi, *J. Taiwan Inst. Chem. Eng.* 63 (2016) 421.
- [26] Y. Yamini, M. Faraji, A.A. Rajabi, F. Nourmohammadian, *Anal. Bioanal. Chem. Res.* 5 (2018) 205.
- [27] S. Lagergren, *Kungliga svenska vetenskapsakademiens Handlingar* 24 (1898) 1.
- [28] Y.-S. Ho, G. McKay, *Process Biochem.* 34 (1999) 451.
- [29] M. Ashrafi, G. Bagherian, M. Arab Chamjangali, N. Goudarzi, *Anal. Bioanal. Chem. Res.* 5 (2018) 95.
- [30] S. Ghassamipour, N. Rostapour, *Anal. Bioanal. Chem. Res.* 4 (2017) 201.
- [31] S. Javinezhad, A. Larki, Y. Nikpour, S.J. Saghanezhad, *Anal. Bioanal. Chem. Res.* 5 (2018) 217.
- [32] Y. Liu, X. Meng, J. Han, Z. Liu, M. Meng, Y. Wang, R. Chen, S. Tian, *J. Sep. Sci.* 36 (2013) 3949.
- [33] G. McKay, *J. Chem. Technol. Biotechnol.* 32 (1982) 759.

- [34] E. Sabah, M. Celik, *J. Colloid Interface Sci.* 251 (2002) 33.
- [35] S. Lazarević, I. Janković-Častvan, V. Djokić, Z. Radovanovic, D. Janačković, R. Petrovic, *J. Chem. Eng. Data* 55 (2010) 5681.
- [36] A. Hosseinifar, M. Shariaty-Niassar, S. Seyyed Ebrahimi, M. Moshref-Javadi, *Langmuir* 33 (2017) 14728.
- [37] S. Dikmen, G. Yilmaz, E. Yorukogullari, E. Korkmaz, *Can. J. Chem. Eng.* 90 (2012) 785.
- [38] S. Veli, B. Alyüz, *J. Hazard. Mater.* 149 (2007) 226.
- [39] S. Duan, R. Tang, Z. Xue, X. Zhang, Y. Zhao, W. Zhang, J. Zhang, B. Wang, S. Zeng, D. Sun, *Colloids Surf., A* 469 (2015) 211.
- [40] S.E. Elaigwu, V. Rocher, G. Kyriakou, G.M. Greenway, *J. Ind. Eng. Chem.* 20 (2014) 3467.
- [41] D. Mohan, H. Kumar, A. Sarswat, M. Alexandre-Franco, C.U. Pittman Jr, *Chem. Eng. J.* 236 (2014) 513.
- [42] M. Yurdakoç, Y. Seki, S. Karahan, K. Yurdakoç, *J. Colloid Interface Sci.* 286 (2005) 440.
- [43] M. Fayazi, M.A. Taher, D. Afzali, A. Mostafavi, M. Ghanei-Motlagh, *Mater. Sci. Eng., C* 60 (2016) 365.
- [44] S.A. Ali, O.C.S. Al Hamouz, N.M. Hassan, *J. Hazard. Mater.* 248 (2013) 47.
- [45] S.N.A. Abas, M.H.S. Ismail, S.I. Siajam, M.L. Kamal, *J. Taiwan Inst. Chem. Eng.* 50 (2015) 182.
- [46] M.A. Salam, *Colloids Surf., A* 419 (2013) 69.
- [47] B. Guo, F. Deng, Y. Zhao, X. Luo, S. Luo, C. Au, *Appl. Surf. Sci.* 292 (2014) 438.
- [48] L. Bo, Q. Li, Y. Wang, L. Gao, X. Hu, J. Yang, *J. Environ. Chem. Eng.* 3 (2015) 1468.
- [49] W. Sun, K. Yin, X. Yu, *Chem. Eng. J.* 225 (2013) 464.
- [50] S. Yang, J. Hu, C. Chen, D. Shao, X. Wang, *Environ. Sci. Technol.* 45 (2011) 3621.
- [51] R. Bai, Y. Zhang, Z. Zhao, Q. Liao, P. Chen, P. Zhao, W. Guo, F. Yang, L. Li, *J. Ind. Eng. Chem.* 59 (2018) 416.
- [52] H.A. Sani, M.B. Ahmad, M.Z. Hussein, N.A. Ibrahim, A. Musa, T.A. Saleh, *Process Saf. Environ. Prot.* 109 (2017) 97.
- [53] P. Pal, S.S. Syed, F. Banat, *J. Water Process Eng.* 20 (2017) 40.
- [54] J. Liu, T. Mwamulima, Y. Wang, Y. Fang, S. Song, C. Peng, *J. Mol. Liq.* 243 (2017) 205.
- [55] R. Fu, Y. Yang, Z. Xu, X. Zhang, X. Guo, D. Bi, *Chemosphere* 138 (2015) 726.
- [56] E. Eren, H. Gumus, *Desalination* 273 (2011) 276.
- [57] L. Kong, Z. Li, X. Huang, S. Huang, H. Sun, M. Liu, L. Li, *J. Mater. Chem. A* 5 (2017) 19333.
- [58] R. Huang, M. Wu, T. Zhang, D. Li, P. Tang, Y. Feng, *ACS Sustainable Chem. Eng.* 5 (2017) 2774.
- [59] H. Asiabi, Y. Yamini, M. Shamsayei, E. Tahmasebi, *Chem. Eng. J.* 323 (2017) 212.